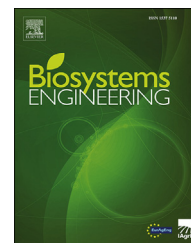


Available online at www.sciencedirect.com

ScienceDirect

journal homepage: www.elsevier.com/locate/issn/15375110

Special Issue: Numerical Tools for Soils

Research Paper

The frequency domain approach to analyse field-scale miscible flow transport experiments in the soils

Gerardo Severino^{a,*}, Gerardo Toraldo^b, Daniel M. Tartakovsky^c^a Department of Agricultural Sciences, University of Naples – Federico II, Italy^b Department of Mathematics and Applications “Renato Caccioppoli”, University of Naples – Federico II, Italy^c Department of Mechanical and Aerospace Engineering, University of California – San Diego, USA

ARTICLE INFO

Article history:

Published online 25 October 2016

keywords:

Solute transport

Frequency domain

Moments

Estimate of parameters

A new approach to the estimate of the parameters u (advective velocity) and λ (dispersivity) characterizing solute transport in soils is presented. The pair (u, λ) is estimated by matching in the *frequency domain* (FD) the theoretical expression of moments pertaining to the *breakthrough curve* (BTC) against to the one evaluated by means of the experimental data. In particular, we demonstrate that to reduce the impact of the random measurement-errors upon such an estimate, it is worth retaining in the Fourier's expansion of the moments only the harmonics associated to the smaller frequencies. This is due to the fact that the Fourier transform moves most of the measurement-errors affecting moments in the high-frequency range. As a consequence, by adopting a relatively small number of harmonics to compute the Fourier transform of the experimental moments, one may filter out most of the noise. It is also shown that the number of harmonics to retain (cut-off) depends upon the soil's water content as well as the magnitude of the characteristic length l_e of the error relative to the dispersivity λ .

The proposed methodology has been applied to a recently conducted plot-scale transport experiment. For comparison purposes, we have also estimated the pair (u, λ) by the classical *method of moments* (MM). Both the methods lead to the same value of the advective velocity u . This is explained by recalling that u depends upon the first-order moment, a quantity that is scarcely influenced by the measurement-errors. Instead, the estimate of the dispersivity λ (which is related to the second-order moment) is largely different (with the value achieved by the MM larger than the one obtained by the FD approach). Such a difference is addressed to the fact that in the MM the distortion-effect due to the measurement-errors amplifies with the increasing order of the moments, a phenomenon which is completely avoided in the FD approach by adopting the above mentioned cut-off.

© 2016 IAGrE. Published by Elsevier Ltd. All rights reserved.

* Corresponding author. Division of Water Resources Management and Biosystems Engineering, via Università 100, 80055, Portici, NA, Italy. Fax: +39 081 2539426(412).

E-mail address: severino@unina.it (G. Severino).<http://dx.doi.org/10.1016/j.biosystemseng.2016.10.002>

1537-5110/© 2016 IAGrE. Published by Elsevier Ltd. All rights reserved.

List of symbols and nomenclature

α	dimensionless parameter
C [$M L^{-2} T^{-1}$]	flux concentration
D [$L^2 T^{-1}$]	dispersion coefficient
δ	Dirac distribution
EP	efficiency parameter
\mathcal{E}_n [$M L^{-2} T^n$]	noise affecting the n -order moment
\tilde{f}	Fourier transform of f
\bar{f}	Laplace transform of f
H	Heaviside step function
K_m	modified m -order Bessel function of the second kind
$\ell_{\mathcal{E}}$ [L]	transverse length scale of the error-measurements
λ [L]	dispersivity
M_0 [$M L^{-2}$]	solute mass per unit area
M_n [$M L^{-2} T^n$]	moment of n -order
$M_n^{(exp)}$ [$M L^{-2} T^n$]	experimental moment of n -order
\mathcal{M}_n	dimensionless moment of n -order
Ω	transport domain
ω [L^{-1}]	spatial frequency
$\bar{\omega}$	dimensionless spatial frequency
q [$L T^{-1}$]	flux
ϑ [$L^3 L^{-3}$]	volumetric water content
ρ [$M L^{-3}$]	soil's bulk density
t [T]	time
t_c [T]	time scale of transport
u [$L T^{-1}$]	advective velocity
u_{eff} [$L T^{-1}$]	effective velocity
\bar{u}_{eff} [$L T^{-1}$]	mean effective velocity
z [L]	depth
ζ	dimensionless depth

1. Introduction

The use of transport experiment(s) as a tool to identify the convective-dispersive properties of soils has been discussed in numerous studies (a wide review can be found in Rubin, 2003, and references therein). Classically, the identification of the transport parameters is carried out by the MM, first introduced by Aris (1958) and subsequently refined by many others (see, e.g. Gómez, Severino, Randazzo, Toraldo, & Otero, 2009; Köhne, Köhne, & Simunek, 2009; Severino, Santini, & Sommella, 2003, and references therein). A drawback related to such an approach is that moments are highly sensitive to their order, and therefore measurement-errors produce an enhancing distortion on the higher-order moments. Nevertheless, the MM is by far the most used method thanks to its ease of implementation. An alternative approach, based upon the Fourier analysis, has been proposed by Duffy and Al-Hassan (1988). In this case, the parameters' estimate is achieved by comparing the theoretical vs experimental BTCs in the FD. Unlike the MM, in the FD approach the dispersion mechanism *de facto* acts as a low pass-filter (Owen, 2007). As a consequence, if one can limit to a relatively small number of harmonics (low frequency range) the numerical computation

of the Fourier transform of the experimental BTCs, then the parameters' estimate would be affected to a much lesser extent by the measurement-errors. One (technical) disadvantage is that the experimental BTCs must be Fourier transformed (by means of the fast Fourier transform). Nevertheless, such a drawback is compensated by the fact that in the FD simple (closed form) solutions are almost always available, whereas in the time domain they may not even exist, or result tremendously cumbersome (see, e.g. Sardin, Schweich, Leij, & Genuchten, 1991; Severino & Indelman, 2004; Severino, Monetti, Santini, & Toraldo, 2006).

So far the FD approach has been used (see e.g. Duffy & Al-Hassan, 1988) to determine the transport parameters at laboratory scale (samples of small sizes), where it is relatively simple to monitor the BTCs. However, at field (and even larger) scales this is not anymore the case due to the numerous limitations mainly related to the heterogeneity, which is a typical feature of the soils at that scale (see, e.g. Coppola et al., 2011; Fiori et al., 2010; Severino & Santini, 2005; Severino, Santini, & Monetti, 2009; Severino & Coppola, 2012; Severino, Tartakovsky, Srinivasan, & Viswanathan, 2012). In this case, the accessible information is the first and second order moment (see, e.g. Severino, Dagan, & van Duijn, 2000, 2007), and consequently the FD approach, as implemented at laboratory scale, does not apply.

Thus, a new approach dealing with moments rather than BTCs is required. To this aim, we refer to the following conditions (typical at field scale): a steady, one-dimensional flow takes place into a semi-bounded domain $\Omega \equiv \{z \in \mathbb{R} : z \geq 0\}$ which is initially solute free, i.e. $C(z, 0) \equiv 0$, being C the flux concentration. A specific (per unit surface) mass M_0 is then applied at the surface $z = 0$ in the form of a pulse, and it is subsequently moved downward by advection. We also assume that at the very deep depths transport is immaterial. These translate into the following boundary conditions

$$C(0, t) = \frac{M_0}{u} \delta(t), \quad \lim_{z \rightarrow \infty} C(z, t) = 0, \quad (1)$$

being u the advective velocity. The n^{th} -order moment writes as:

$$M_n(z) = \int_0^\infty dt t^n C(z, t), \quad z \in \Omega. \quad (2)$$

Thus, if the concentration $C \equiv C(z, t)$ is determined in analytical form, one can compute (either analytically or numerically) moments (2). For the problem at stake, the concentration is obtained by solving (for details, see e.g. Jury & Roth, 1990, ch. 2.5.2) the advection-dispersion equation:

$$\frac{\partial}{\partial t} C + u \frac{\partial}{\partial z} C = D \frac{\partial^2}{\partial z^2} C \quad (3)$$

under the above initial/boundary conditions, the final result being:

$$C(z, t) = \frac{M_0 z}{2t\sqrt{\pi Dt}} \exp \left[- \left(\frac{z - ut}{2\sqrt{Dt}} \right)^2 \right]. \quad (4)$$

The dispersion coefficient D encompasses both diffusion and dispersive mechanisms, although the latter are always prevailing upon the former (a wide discussion upon such an

interplay of mechanisms can be found in [Bellin, Severino, & Fiori, 2011](#)). This is particularly so when one is interested into computing moments, and therefore we adopt such an assumption hereafter. Thus, with the neglect of the diffusion one can relate D to the so called dispersivity λ as $D \sim \lambda u$ ([Bear, 2013](#)). Insertion of (4) into (2) leads, after computing the integral, to

$$M_n(z) = M_0 \sqrt{\frac{z}{\pi\lambda}} \left(\frac{z}{u}\right)^n \exp\left(\frac{z}{2\lambda}\right) K_{n-1/2}\left(\frac{z}{2\lambda}\right) \quad (n = 1, 2, \dots), \quad (5)$$

where $K_m(x)$ is the modified m -order Bessel function of the second kind ([Abramowitz & Stegun, 1964](#)). The non dimensional moments:

$$\mathcal{M}_n(\zeta) \equiv \frac{M_n}{M_0} \left(\frac{u}{\lambda}\right)^n = \frac{\zeta^{n+1/2}}{\pi^{1/2}} \exp(\zeta/2) K_{n-1/2}(\zeta/2) \quad (n = 1, 2, \dots) \quad (6)$$

have been depicted in [Fig. 1](#) as function of the scaled depth $\zeta \equiv z/\lambda$, and a few values of the order n . The important feature is that moments are highly sensitive to n , and therefore higher order moments ($n \geq 2$) are strongly influenced by the fluctuations induced by the measurement-errors.

2. Mathematical formulation of the problem

To minimise as much as possible the impact of the measurement-errors in the identification of the parameters, we employ an alternative methodology based upon the FD approach. Toward this aim in the sequel we present the theoretical background related to the implementation of such an approach. Central for our methodology is the Laplace transform of the n -order moment, i.e.

$$\bar{M}_n(s) = \int_0^\infty dz M_n(z) \exp(-sz). \quad (7)$$

To compute \bar{M}_n it was found easier from the mathematical point of view to deal with the moments' equation, which is obtained by multiplying both sides of (3) by t^n and integrating over t (and employing integration by parts), i.e.

$$D \frac{d^2}{dz^2} M_n(z) - u \frac{d}{dz} M_n(z) + n M_{n-1}(z) = 0, \quad (n = 1, 2, \dots) \quad (8)$$

with $M_0(z) \equiv M_0$. The boundary conditions for the ODE (8) are easily obtained from (1) as follows:

$$\begin{aligned} M_n(0) &= \int_0^\infty dt t^n C(0, t) = \frac{M_0}{u} \int_0^\infty dt t^n \delta(t) = 0, \quad M_n(\infty) \\ &= \lim_{z \rightarrow \infty} \int_0^\infty dt t^n C(z, t) = 0 \end{aligned} \quad (9)$$

(any $n \geq 1$). Application of the Laplace transform (7) to eq. (8) yields:

$$\bar{M}_n(s) = \frac{\lambda u M'_n(0) - n \bar{M}_{n-1}(s)}{us(\lambda s - 1)}, \quad n = 1, 2, \dots \quad (10)$$

(where we have accounted for $D \sim \lambda u$). In particular, from (5) one has $M'_1(0) = M_0/u$ and $M'_2(0) = 2M_0\lambda/u^2$, and therefore the Laplace transform of the first and second order moment writes as:

$$\bar{M}_1(s) = \frac{M_0}{us^2}, \quad \bar{M}_2(s) = \frac{2M_0}{u^2 s^3} (\lambda s + 1). \quad (11)$$

Hence, in the FD approach the pair (u, λ) is identified by minimizing the distance between the theoretical moments (11) and those (say $\bar{M}_n^{(exp)}$) estimated via the miscible transport experiment(s), i.e.

$$\min_{u, \lambda} \left| \bar{M}_n(s) - \bar{M}_n^{(exp)}(s) \right|, \quad (n = 1, 2). \quad (12)$$

The crux of the matter is now to relate $\bar{M}_n^{(exp)}$ to the Fourier transform in order to compute the discrete Laplace transform

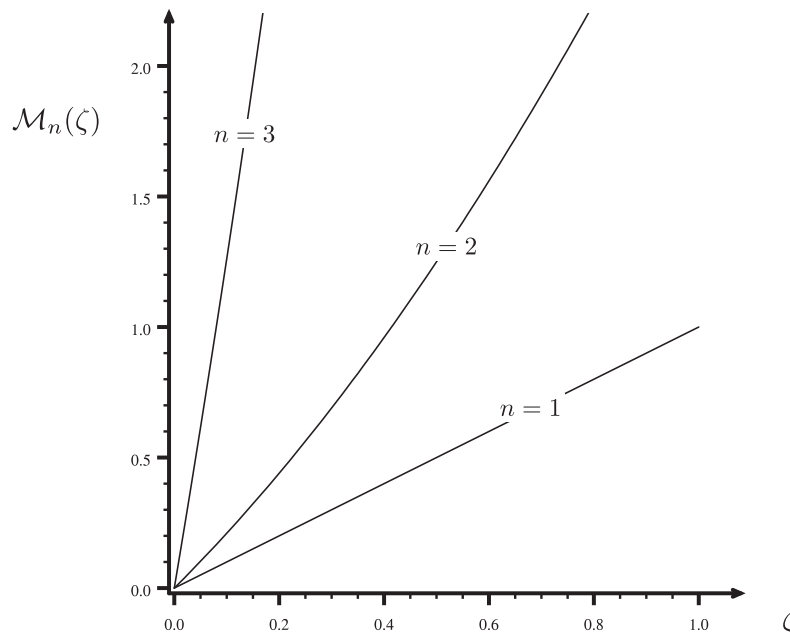


Fig. 1 – Normalised moments $\mathcal{M}_n(\zeta)$ versus the scaled depth ζ for different values of the order n .

by means of the fast Fourier transform (Poularikas, 2010; Press, Teukolsky, Vetterling, & Flannery, 1996). Toward this aim, we first note that the Laplace transform $\bar{M}_n(s)$ of the moments can be expressed via the Fourier transform (spectrum)

$$\tilde{f}(\omega) = \int_{\mathbb{R}} dx f(x) \exp(i\omega x) \quad \text{for any } f(x) \in \mathcal{L}(\mathbb{R}) \quad (13)$$

by the straightforward relationship $\tilde{M}_n(\omega) \equiv \bar{M}_n(-i\omega)$. This latter is easily proved after noting that

$$\begin{aligned} \bar{M}_n(-i\omega) &= \int_0^\infty dz M_n(z) \exp(i\omega z) \\ &= -\frac{1}{\omega} \int_{\mathbb{R}} dz H(z) M_n(z) \frac{d}{dz} \exp(i\omega z), \end{aligned} \quad (14)$$

and carrying out integration by parts (H is the Heaviside step-function).

We now decompose the experimental moment $M_n^{(\text{exp})}$ as a sum of the true one, M_n , and a noise, ε_n , i.e.

$$M_n^{(\text{exp})}(z) = M_n(z) + \varepsilon_n(z), \quad (15)$$

and we aim at estimating M_n from $M_n^{(\text{exp})}$ in the presence of ε_n . This is a difficult task, and some additional *a priori* information (or assumption) concerning the shape of ε_n as well as its correlation with M_n is required. In particular, we shall assume in line with the standard approach of the signal processing theory (see, e.g. Owen, 2007) that M_n and ε_n are uncorrelated. This leads to

$$\left| \tilde{M}_n^{(\text{exp})}(\omega) \right|^2 = \left| \tilde{M}_n(\omega) \right|^2 + \left| \tilde{\varepsilon}_n(\omega) \right|^2. \quad (16)$$

As a consequence, for a transport experiment one can calculate the whole spectrum $\tilde{M}_n^{(\text{exp})}$, and subsequently separate the true spectrum, \tilde{M}_n , from the noise one, $\tilde{\varepsilon}_n$, by comparing with the right hand side of (16). In the present study, we consider the case of a “white-noise” process for ε_n , i.e.

$$\varepsilon_n(z) \approx \mathcal{S}_n \delta(z), \quad 0 < \mathcal{S}_n \equiv \text{constant}, \quad (17)$$

and, we limit our analysis to $n = 1, 2$ (since the first and second order moments are of relevance for the study at stake). Hence, from (11) one has:

$$\begin{aligned} \left| \tilde{M}_1^{(\text{exp})}(\omega) \right|^2 &= \left(\frac{M_0}{u} \right)^2 \omega^{-4} + \mathcal{S}_1^2, \quad \left| \tilde{M}_2^{(\text{exp})}(\omega) \right|^2 \\ &= 4 \left(\frac{M_0}{u^2} \right)^2 \frac{1 + (\lambda\omega)^2}{\omega^6} + \mathcal{S}_2^2. \end{aligned} \quad (18)$$

Inspection of (18) clearly shows that the noise-spectrum (\mathcal{S}_1 and \mathcal{S}_2 in the present study) is nearly flat. To the contrary, the spectral signature of the true process is practically concentrated in the low frequency range where it exhibits a very well distinguished increase. As a consequence, within the low frequency range one has $\left| \tilde{M}_n \right|^2 \gg \left| \tilde{\varepsilon}_n \right|^2$, and concurrently the true signal $M_n^{(\text{exp})}$ practically coincides with the theoretical one M_n .

To illustrate the utility of the present study to design a sampling strategy to minimise the measurement-errors, we have depicted in Fig. 2 the scaled spectrum $\left| \tilde{M}_2^{(\text{exp})} \right|^2 / \mathcal{S}_2^2$ versus the dimensionless (spatial) frequency $\bar{\omega} = \lambda\omega$, and some values of the parameter $\alpha = M_0 \lambda^3 / (\mathcal{S}_2 u^2)$. First, it is seen that the measurements coincide with the true signal within the “low frequency-range”, and this explains why only a relatively small number (usually between 5 and 8) of harmonics in the fast Fourier transform is required in order to filter out most of the measurement-errors (see, e.g. discussion in Duffy & Al-Hassan, 1988, and references therein). In particular, the smaller is α the larger is the impact of the measurement-error (and concurrently the poor is the agreement between theoretical and true moments), and *viceversa*. To illustrate how to obtain a relatively large frequency range (and therefore to design a proper sampling spatial grid) where $M_2^{(\text{exp})} \approx M_2$, it is worth noting that $M_0 / \mathcal{S}_2 \sim (t_c^2 \ell_\varepsilon)^{-1}$, being t_c and ℓ_ε the transport time scale and a characteristic (transverse) length scale of the measurement-errors, respectively. By noting that a typical time scale of transport is λ/q , one has $\alpha \approx \vartheta^2 (\lambda / \ell_\varepsilon)$. As a consequence, increasing the range of frequency where $M_2^{(\text{exp})} \approx M_2$ (Fig. 2) is determined by: either i) large water content values (i.e. when ϑ is closer the water content at the saturation), or ii) by a transport process whose dispersivity λ overtakes the transverse length scale ℓ_ε of the measurement-errors, somewhat similar to the ergodicity attainment in the stochastic approach to solute transport in heterogeneous porous media (Dagan, 1991; Severino, Santini, & Sommella, 2011). In the sequel, we apply our theoretical results to a recently conducted field-scale transport experiment.

2.1. The transport experiment

To illustrate the potential of our procedure toward the estimate of the transport parameters (u, λ), we refer to a miscible transport experiment that has been recently conducted. The experiment is described in detail by Severino, Comegna, Coppola, Sommella, and Santini (2010). For the purposes of the present study, it is summarised briefly herein.

The site is located at Ponticelli (Naples, Italy). The analysis of the texture from $z = 0$ to $z = 100$ cm suggests that the soil is a moderately structureless sand (relative coarse-texture) till to $z \leq 80$ cm, and loam (fine-texture) for $80 \leq z \leq 100$ cm with bulk density $\rho = (1.0 \pm 0.1) \text{ g cm}^{-3}$. A plot, 8 m (width) \times 50 m (long), was set-up in a greenhouse equipped with an irrigation (sprinkler-type) system. Prior to the solute application, the plot was irrigated ($q = 4.2 \cdot 10^{-2} \text{ cm h}^{-1}$) with fresh water to achieve a steady water content $\vartheta = 0.33 \pm 0.04$ (for details, see Severino, Comegna, & Sommella, 2005a; Comegna, Severino, & Sommella, 2006b). Then, a pulse of chloride (KCl) was applied at the surface ($M_0 = 105 \text{ g m}^{-2}$), and subsequently leached till to $z = 200$ cm by irrigating with the same flux q applied before the application of the chloride (see, e.g. Coppola et al., 2004; Comegna, Severino, & Sommella, 2006a).

Monitoring the Cl-concentration was intensively carried out (for details, see Severino et al., 2010) at several depths (i.e.

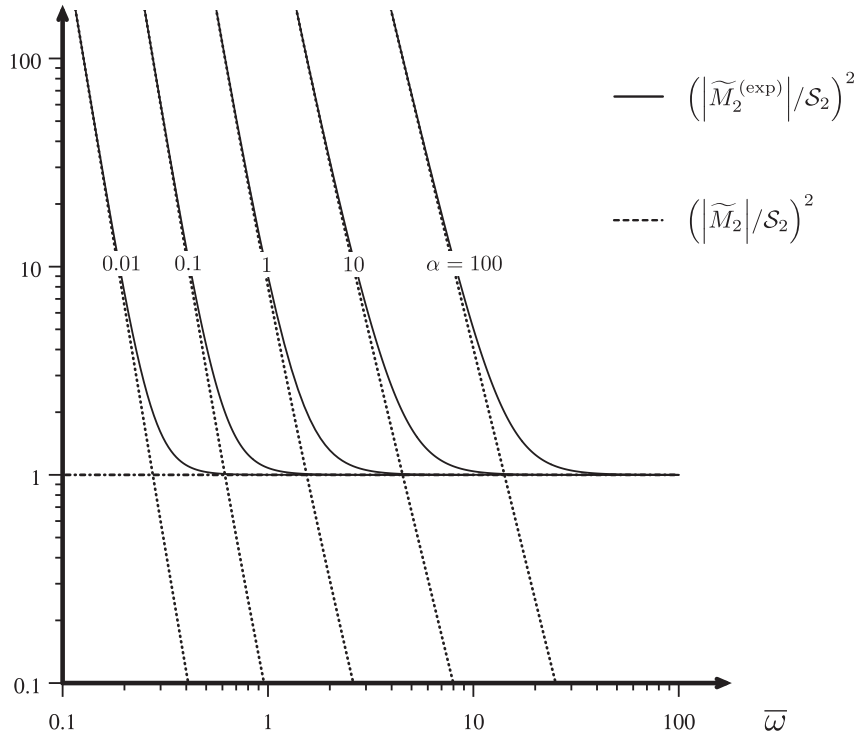


Fig. 2 – The scaled (continuous lines) spectrum $(|\tilde{M}_2^{(\text{exp})}|/\mathcal{S}_2)^2$ as function of the dimensionless frequency $\bar{\omega} = \lambda \omega$, and different values of $\alpha \equiv M_0 \lambda^3 / (\mathcal{S}_2 u^2)$. The dashed lines pertain to the spectrum $(|\tilde{M}_2|/\mathcal{S}_2)^2$ of the scaled true signal.

$z = 5, 15, 25, 35, 45, 55, 65, 75, 85$ cm), and most of the corresponding BTCs are shown in Fig. 3. In fact, due to some logistic problems occurred during the experiment, the recovery mass at $z = 65$ cm and $z = 85$ cm was very poor, and therefore meaningless for the purposes of the present study. As a consequence, we did not consider the BTCs at these two depths. It is seen that the peak of the concentration decreases with increasing depth, therefore suggesting a significant impact of the dispersion mechanism (which strictly depends upon the second order moment). As we have already pointed out, the accessible information in such situations is just the pair (M_1, M_2) . Instead, in the case of the Ponticelli-experiment we also have the BTCs which we shall use as benchmark. This further underpins (among the others) the uniqueness of the Ponticelli transport experiment.

In the sequel we shall apply both the MM and the FD-approach in order to discuss the performance of each method into properly reproducing the experimental BTCs of Fig. 3. Before proceeding further it is worth recalling here that in the MM, and for a pulse-like (ideal) boundary condition, one relates the first and second order moments (2) to the transport parameters u and λ via the relations:

$$u \equiv \frac{z}{\mathcal{T}}, \quad \lambda \equiv \frac{\xi}{2} z \quad (19)$$

(see, e.g. Jury & Roth, 1990), being $\mathcal{T} = M_1/M_0$ and $\xi = M_2/(M_0 M_1^2) - 1$. Hence, once the moments are estimated by means of the miscible transport experiment(s), one can easily determine the advective velocity and the dispersivity via eq (19). If the boundary conditions differ from the ideal ones, one

can modify this formulation to come up with a similar couple of relationships (see, e.g. Ojha, Prakash, Corradini, Morbidelli, & Govindaraju, 2015).

3. Discussion

As a first step, we have calibrated the transport equation (3) at $z = 55$ cm by means of both the MM and the FD approach. In particular, the latter task was achieved by taking the first 8 harmonics to compute the fast Fourier transform. The choice of such a depth for calibration purposes is dictated by the need to minimise the impact of the upper boundary condition, which is well known to prevent (due to the nonuniformities in the water/solute application) adoption of the advection-dispersion equation (see e.g. discussion in Comegna, Coppola, & Sommella, 1999; Coppola, Comegna, Basile, Lamaddalena, & Severino, 2009, 2011; Severino et al., 2009). The resulting calibration-values are summarised in the Table 1.

It is seen that the two methods lead to the same advective velocity u . This was somehow expected since u is related to the first-order moment (19), and therefore its estimate is scarcely sensitive to the enhancing effect of the error/uncertainties in the measurements. It also should be noted that the mean effective velocity $\bar{u}_{\text{eff}} (\text{cm h}^{-1}) \equiv q/\bar{\vartheta} = 0.042/0.33 = 13 \cdot 10^{-2} \text{ cm h}^{-1}$, obtained via the applied flux q and the mean water content $\bar{\vartheta}$, is slightly smaller than u . This is presumably addressed to the larger variations of ϑ due to the vertical heterogeneities of the soil at the plot scale (Severino et al., 2010). Nevertheless, since the standard deviation of the water content

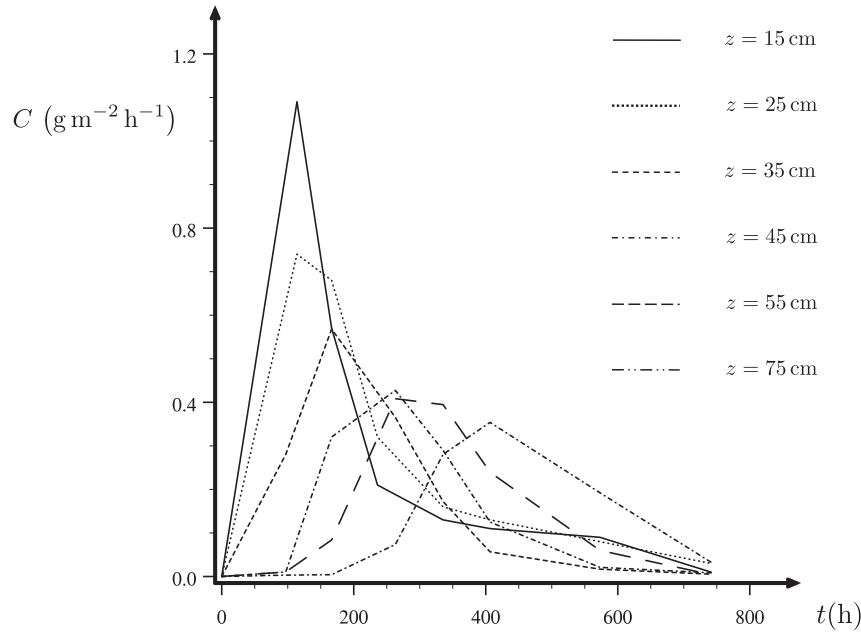


Fig. 3 – Experimental BTCs of the chloride at the sampling depths along the plot at the Ponticelli-site.

is $\sigma_{\vartheta} = 0.04$ (see the above description of the transport experiment), one has:

$$u_{\text{eff}} = \bar{u}_{\text{eff}} + \sigma_{u_{\text{eff}}} \frac{q}{\vartheta} = \frac{4.2 \cdot 10^{-2}}{0.33 \pm 0.04} \text{ cm h}^{-1} \approx (13 \pm 2) \cdot 10^{-2} \text{ cm h}^{-1}, \tag{20}$$

and concurrently the discrepancy between \bar{u}_{eff} and u can be explained by the range of variability of the water content. This also confirms that the resulting variability in the estimated advection velocity is actually a measure of the hydraulic properties relevant for the experiment at stake, and not an artifact of the method(s) of estimate.

The solute spreading, that is related to the second-order moment, is accounted by the characteristic dispersivity length λ . Unlike the advection, the estimate of λ based upon the MM is higher than the one obtained by the FD approach (Table 1). A first explanation is that the MM is highly sensitive to the large spreading of the BTCs close to the upper boundary (for details, see Press et al., 1996) due to the large variability of u (it is reminded that $D \sim \lambda u$) in the close vicinity of $z = 0$ (Severino et al., 2010). Another way to address to such a difference is to invoke an “additional” dispersion mechanism such as retardation and/or diffusion into immobile regions. However, this would require a completely different model accounting simultaneously for migration from/toward zones of stagnation within the porous medium, a task which is left to future studies.

Table 1 – Transport parameters u and $\lambda \equiv D/u$ pertaining to the model (3) as calibrated at the depth $z = 55$ cm by the MM, and the FD approach.

MM		FD	
u (cm h ⁻¹)	λ (cm)	u (cm h ⁻¹)	λ (cm)
$15 \cdot 10^{-2}$	4.3	$15 \cdot 10^{-2}$	3.0

In Fig. 4 we have depicted the theoretical BTCs-(4) as calibrated by means of the MM (dashed line), and the FD approach (continuous lines) along with the experimental BTCs (symbols). The better agreement between the BTCs calibrated by the FD approach is quantitatively confirmed (see Table 2) by the efficiency parameter (EP)

$$EP = 1 - \frac{\sum_{i=1}^n [C_i^{(\text{mod})} - C_i^{(\text{exp})}]^2}{\sum_{i=1}^n [\bar{C} - C_i^{(\text{exp})}]^2}, \quad \bar{C} = \frac{1}{n} \sum_{i=1}^n C_i^{(\text{exp})}, \tag{21}$$

where $C_i^{(\text{mod})}$ and $C_i^{(\text{exp})}$ represent modelled and measured concentrations, respectively.

Before concluding, we wish to comment the significance of the result $\lambda \sim \text{constant}$ for $35 \text{ cm} \leq z \leq 75 \text{ cm}$. Indeed, a propagation process which is characterised by a constant dispersivity is typical of an advection-dispersion mechanism (Fickian transport). To the contrary, in the shallowest depths ($z \leq 25 \text{ cm}$) the process is not anymore Fickian, and therefore another modelling approach (along the lines suggested by Severino, Cvetkovic, & Coppola, 2005b; Severino & Coppola, 2012) would be more appropriate.

4. Concluding remarks

In the present study the FD approach to estimate the transport parameters (u , λ) pertaining to the advection-dispersion equation (3) is considered. For comparison purposes the FD approach and the MM were applied to a recently conducted field scale miscible transport experiment. The two methods were found to provide the same value of the advective term u ; instead, they lead to considerably different λ -values. Such a difference is attributed to the “building up effect” of measurement-errors generated by the MM. In particular, we

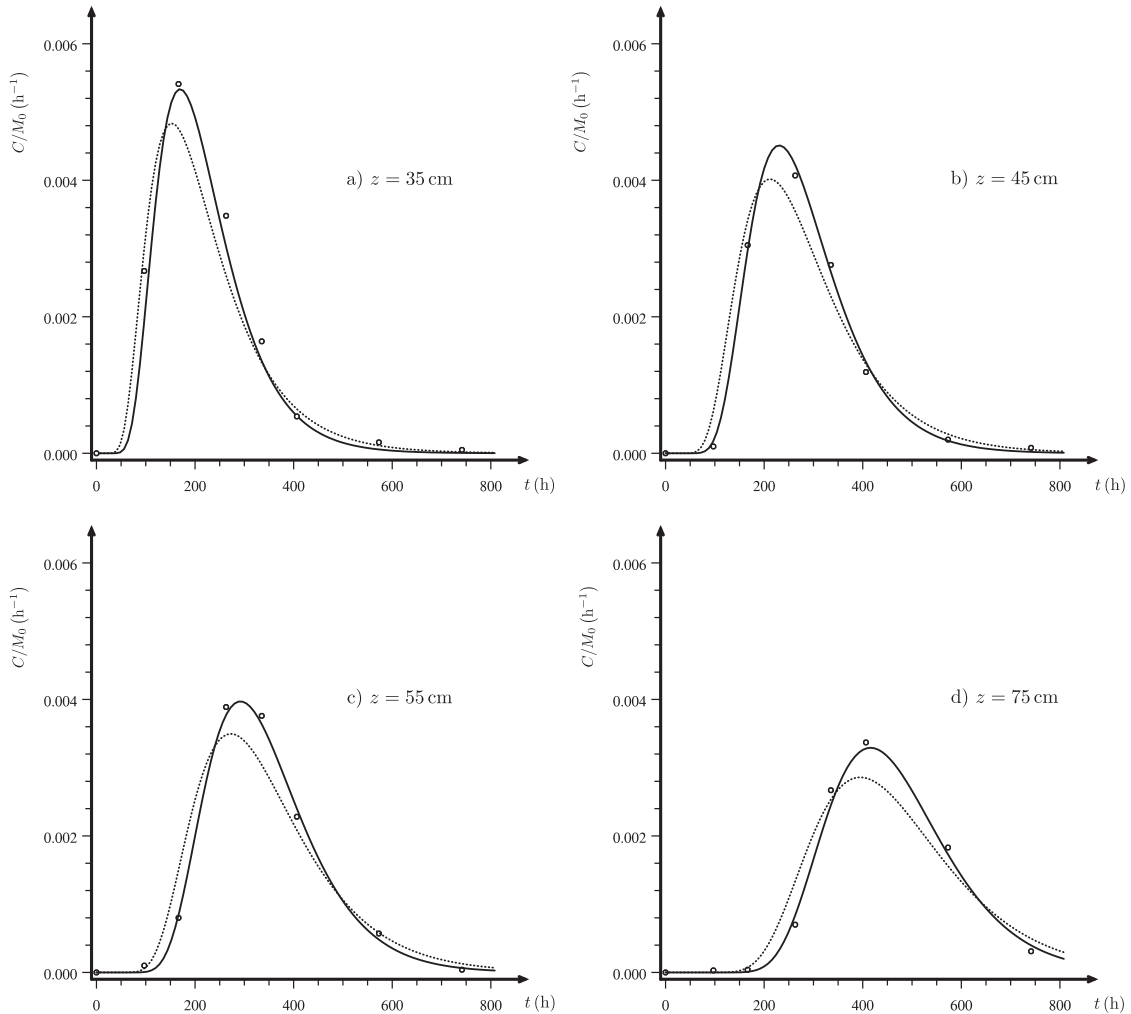


Fig. 4 – Scaled BTCs C/M_0 (h^{-1}) versus the elapsed time t (h) at $z = 35, 45, 55,$ and 75 cm. The dashed lines refer to the BTCs as determined by the MM, whereas continuous lines pertain to the BTCs determined by the FD approach. Dots indicate the experimental BTCs.

show that the estimate of (u, λ) achieved by the FD approach provides a much better agreement between theoretical and measured BTCs. This is explained by recalling that the FD approach seeks for (u, λ) to honour (12), and therefore it requires that moments are Fourier transformed. Such a transform moves most of the measurement-errors to the high-frequency range and therefore, by adopting a relatively small number of harmonics (8 in the present study) to compute the fast Fourier transform of the experimental moments, one comes up with an estimate of the transport

parameters which is much lesser affected by measurement-errors. Based on this, we have also discussed how to properly design the experimental campaigns in order to minimise the impact of the measurement-errors.

The results of the present study rely upon the assumption that the measurement-errors are concentrated in the close vicinity of the soil surface ($z = 0$), and this justifies modelling ε_n as a white-noise (Dirac distribution). Of course, this is not anymore the case when the noise is coloured, and concurrently another functional model for ε_n has to be adopted. For example, if the noise is “uniformly” distributed from the soil surface $z = 0$ till to the sampling depth $z = z_s$, one has

$$|\tilde{\varepsilon}_n(\omega)|^2 \sim \left(\frac{\sin \omega}{\omega}\right)^2, \quad (22)$$

being $\bar{\omega} \equiv \omega z_s / 2$. In this case, it is seen (Fig. 5) that the frequencies ω_k corresponding to zero $|\tilde{\varepsilon}_n|$ are $\omega_k = 2k\pi/z_s$ (with $k \in \mathbb{N}$). Thus, the stringent result is that, unlike our study, in this case the set of frequencies to consider when computing the fast Fourier transform of the experimental moments is

Table 2 – The efficiency parameter EP (%) pertaining to the: i) MM, and ii) FD approach at the sampling depths shown in Fig. 3.

z (cm)	EP (%)	
	MM	FD
35	94.8	96.4
45	93.3	98.6
55	93.1	99.7
75	93.2	99.2

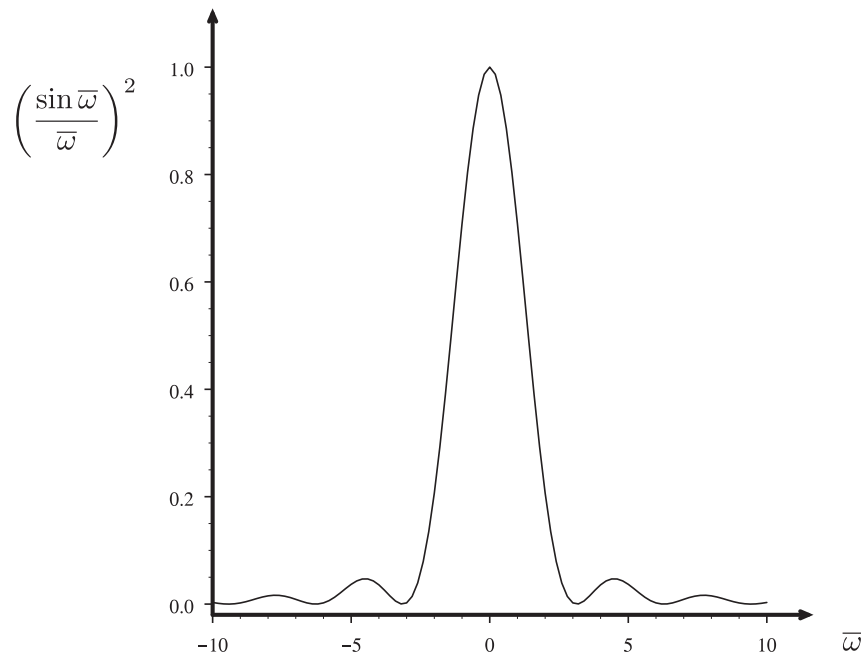


Fig. 5 – Dependence of the function $(\sin^2 \bar{\omega}) / \bar{\omega}^2$ upon the dimensionless frequency $\bar{\omega} \equiv \omega z_s / 2$.

“discrete”. In particular, it is reasonable to limit to $k = 1, 2, 3$ to filter out most of the noise.

This example shows that, depending upon the structure of the noise distribution, both the number and the type of the frequencies to consider in the identification of the transport parameters may significantly change, as consequence of the soil's structure. Before concluding, we wish to underline that when the sampling depth $z \equiv z_s$ is very deep, it turns out that $\omega_k \rightarrow 0$, and concurrently in this case assuming $\mathcal{E}_n \sim \delta$ allows one to account simultaneously for uncertainties due to: i) the spatial variability of the transport parameters (coloured noise), and ii) the measurement-errors at the soil surface (white noise).

Acknowledgements

The first author acknowledges support from “Programma di scambi internazionali per mobilità di breve durata” (Naples University, Italy), “OECD Cooperative Research Programme: Biological Resource Management for Sustainable Agricultural Systems” (Contract No. JA00073336). The very constructive comments and suggestions from the Editor and two anonymous Referees were deeply appreciated.

REFERENCES

- Abramowitz, M., & Stegun, I. A. (1964). *Handbook of mathematical functions: With formulas, graphs, and mathematical tables* (Vol. 55). Courier Corporation.
- Aris, R. (1958). On the dispersion of linear kinematic waves. In *Proceedings of the royal society of london A: Mathematical, physical and engineering sciences, the royal society* (pp. 268–277).
- Bear, J. (2013). *Dynamics of fluids in porous media*. Courier Corporation.
- Bellin, A., Severino, G., & Fiori, A. (2011). On the local concentration probability density function of solutes reacting upon mixing. *Water Resources Research*, 47.
- Comegna, V., Coppola, A., & Sommella, A. (1999). Nonreactive solute transport in variously structured soil materials as determined by laboratory-based time domain reflectometry (TDR). *Geoderma*, 92, 167–184.
- Comegna, A., Severino, G., & Sommella, A. (2006a). Local-scale solute transport in variously structured soils under continuous flood irrigation. In Lorenzini, & Brebbia (Eds.), Vol. 96. *Sustainable irrigation management, technologies and policies*, WIT trans. Ecol. Environ (pp. 85–100).
- Comegna, A., Severino, G., & Sommella, A. (2006b). Surface measurements of hydraulic properties in an irrigated soil using a disc permeameter. In Lorenzini, & Brebbia (Eds.), Vol. 96. *Sustainable irrigation management, technologies and policies*, WIT trans. Ecol. Environ (pp. 341–353).
- Coppola, A., Comegna, V., Basile, A., Lamaddalena, N., & Severino, G. (2009). Darcian preferential water flow and solute transport through bimodal porous systems: Experiments and modelling. *Journal of Contaminant Hydrology*, 104, 74–83.
- Coppola, A., Comegna, A., Dragonetti, G., Dyck, M., Basile, A., Lamaddalena, N., et al. (2011). Solute transport scales in an unsaturated stony soil. *Advances in Water Resources*, 34, 747–759.
- Coppola, A., Santini, A., Botti, P., Vacca, S., Comegna, V., & Severino, G. (2004). Methodological approach for evaluating the response of soil hydrological behavior to irrigation with treated municipal wastewater. *Journal of Hydrology*, 292, 114–134.
- Dagan, G. (1991). Dispersion of a passive solute in non-ergodic transport by steady velocity fields in heterogeneous formations. *Journal of Fluid Mechanics*, 233, 197–210.
- Duffy, C. J., & Al-Hassan, S. (1988). The time and frequency response of tracer experiments. *Journal of Hydrology*, 97, 59–73.
- Fiori, A., Boso, F., de Barros, F. P., De Bartolo, S., Frampton, A., Severino, G., et al. (2010). An indirect assessment on the

- impact of connectivity of conductivity classes upon longitudinal asymptotic macrodispersivity. *Water Resources Research*, 46.
- Gómez, S., Severino, G., Randazzo, L., Toraldo, G., & Otero, J. (2009). Identification of the hydraulic conductivity using a global optimization method. *Agricultural Water Management*, 96, 504–510.
- Jury, W. A., & Roth, K. (1990). *Transfer functions and solute movement through soil: Theory and applications*. Birkhäuser Verlag.
- Köhne, J. M., Köhne, S., & Simunek, J. (2009). A review of model applications for structured soils: Water flow and tracer transport. *Journal of Contaminant Hydrology*, 104, 4–35.
- Ojha, R., Prakash, A., Corradini, C., Morbidelli, R., & Govindaraju, R. S. (2015). Temporal moment analysis for stochastic-advective vertical solute transport in heterogeneous unsaturated soils. *Journal of Hydrology*, 521, 261–273.
- Owen, M. (2007). *Practical signal processing*. Cambridge University Press.
- Poularikas, A. D. (2010). *Transforms and applications handbook*. CRC press.
- Press, W. H., Teukolsky, S. A., Vetterling, W. T., & Flannery, B. P. (1996). *Numerical recipes in C*. Cambridge.
- Rubin, Y. (2003). *Applied stochastic hydrogeology*. Oxford: Oxford University Press.
- Sardin, M., Schweich, D., Leij, F., & Genuchten, M. T. (1991). Modeling the nonequilibrium transport of linearly interacting solutes in porous media: A review. *Water Resources Research*, 27, 2287–2307.
- Severino, G., Comegna, A., Coppola, A., Sommella, A., & Santini, A. (2010). Stochastic analysis of a field-scale unsaturated transport experiment. *Advances in Water Resources*, 33, 1188–1198.
- Severino, G., Comegna, A., & Sommella, A. (2005a). Analytical model for gravity-driven drainage. In Nützmänn, Viotti, & Aagaard (Eds.), *Reactive transport in soil and groundwater: Processes and models* (pp. 209–217).
- Severino, G., & Coppola, A. (2012). A note on the apparent conductivity of stratified porous media in unsaturated steady flow above a water table. *Transport in Porous Media*, 91, 733–740.
- Severino, G., Cvetkovic, V., & Coppola, A. (2005b). On the velocity covariance for steady flows in heterogeneous porous formations and its application to contaminants transport. *Computational Geosciences*, 9, 155–177.
- Severino, G., Cvetkovic, V., & Coppola, A. (2007). Spatial moments for colloid-enhanced radionuclide transport in heterogeneous aquifers. *Advances in Water Resources*, 30, 101–112.
- Severino, G., Dagan, G., & van Duijn, C. (2000). A note on transport of a pulse of nonlinearly reactive solute in a heterogeneous formation. *Computational Geosciences*, 4, 275–286.
- Severino, G., & Indelman, P. (2004). Analytical solutions for reactive transport under an infiltration–redistribution cycle. *Journal of Contaminant Hydrology*, 70, 89–115.
- Severino, G., Monetti, V., Santini, A., & Toraldo, G. (2006). Unsaturated transport with linear kinetic sorption under unsteady vertical flow. *Transport in Porous Media*, 63, 147–174.
- Severino, G., & Santini, A. (2005). On the effective hydraulic conductivity in mean vertical unsaturated steady flows. *Advances in Water Resources*, 28, 964–974.
- Severino, G., Santini, A., & Monetti, V. M. (2009). Modelling water flow water flow and solute transport in heterogeneous unsaturated porous media. In *Advances in modeling agricultural Systems* (pp. 361–383). Springer.
- Severino, G., Santini, A., & Sommella, A. (2003). Determining the soil hydraulic conductivity by means of a field scale internal drainage. *Journal of Hydrology*, 273, 234–248.
- Severino, G., Santini, A., & Sommella, A. (2011). Macrodispersion by diverging radial flows in randomly heterogeneous porous media. *Journal of Contaminant Hydrology*, 123, 40–49.
- Severino, G., Tartakovsky, D., Srinivasan, G., & Viswanathan, H. (2012). Lagrangian models of reactive transport in heterogeneous porous media with uncertain properties. In , Vol. 468. *Proceedings of the royal society of london A: Mathematical, physical and engineering sciences* (pp. 1154–1174).